様　式　Ｃ－１９、Ｆ－１９－１、Ｚ－１９　（共通）

科学研究費助成事業　　研究成果報告書

令和　元 年　 ６ 月　 ５ 日現在

機関番号：１１３０１
研究種目：研究活動スタート支援
研究期間：2017～2018
課題番号：１７Ｈ０６５１１

研究課題名（和文）TAILORING SPIN-ORBIT INTERACTIONS FOR NEUROMORPHIC COMPUTING WITH MAGNETIC DOMAIN WALL MOTION

研究課題名（英文）TAILORING SPIN-ORBIT INTERACTIONS FOR NEUROMORPHIC COMPUTING WITH MAGNETIC DOMAIN WALL MOTION

研究代表者
ＤＵＴＴＡＧＵＰＴＡ　ＳＡＭＩＫ（DUTTAGUPTA, SAMIK）

東北大学・スピントロニクス学術連携研究教育センター・助教

研究者番号：３０８０７６５７

交付決定額（研究期間全体）：（直接経費）　　2,300,000円

研究成果の概要（和文）：本研究課題では反強磁性ヘテロ構造におけるスピン軌道相互作用に関する理解を促進し、不揮発メモリや脳型情報処理に向けた基盤を構築することを目指した。反強磁性／強磁性ヘテロ構造におけるスピン軌道相互作用を利用した強磁性体の磁化の制御方法や、反強磁性／非磁性ヘテロ構造における反強磁性体のネールベクトルの電流制御に関して、これまで知られていなかった現象を観測し、系統的な測定からその物理的機構に関する理解を深めることができた。

研究成果の学術的意義や社会的意義
Quantification of spin-orbit interactions (SOI) in antiferromagnet (AFM)/ferromagnet (FM) enables quantification of physics concerning SOIs and provides insights for design of AFM/FM device. Demonstration of electrical control of AFM-based structures initiates new directions in AFM spintronics.

研究成果の概要（英文）：The current research project deals with the utilization of antiferromagnet-based heterostructures for next generation non-volatile and neuromorphic computing architectures. The first part of the project clarified the role of spin-orbit interactions in antiferromagnet (AFM)/ferromagnet heterostructures which is considered to be a promising building block for future spintronic devices. The obtained information provides crucial insights for design of device structure using AFM/FM. The second part of the project takes a further step ahead towards the realization of pure AFM based spintronic architectures for antiferromagnetic spintronics. We have demonstrated electrical reading and writing of a metallic AFM by spin-orbit torques originating from the injection of current in an adjacent non-magnet layer with strong spin-orbit interactions. The obtained results offer an unexplored pathway for the development of next generation spintronic devices utilizing antiferromagnetic materials.

研究分野：Antiferromagnetic Spintronics

キーワード：Antiferromagnet　Neuromorphic Computing　Spin-orbit interactions

１．研究開始当初の背景

The future of electronics is gradually inclined towards the realization of nueromorphic computing for high-performance and intelligent computing architectures. The utilization of spin, charge and orbital degrees of freedom of electron is expected to enhance the efficiency of spintronic device architectures. In our previous work, we have demonstrated current-induced magnetization switching in antiferromagnet (AFM)-based AFM/ferromagnet (FM) structure proceeding in an memristive manner rendering a promising building block for spintronics-based neuromorphic computing device architectures [1-3].

２．研究の目的

Antiferromagnetic heterostructures with broken inversion symmetry are perceived to open new opportunities for non-volatile spintronics-based neuromorphic computing architectures. The presence of spin-orbit interactions in AFM-based heterostructures results in drastic ramifications, requiring deeper understanding towards their utilization in neuromorphic computing architectures. The injection of an in-plane current in AFM/FM heterostructures with strong spin-orbit coupling and broken inversion symmetry results in spin-orbit torques (SOTs), which allows manipulation of magnetization and/or efficient domain-wall (DW) motion in the adjacent ferromagnetic layer. Furthermore, the injection of current generates Néel SOTs which is capable of manipulation and/or DW motion in the AFM itself. The successful utilization of AFM-based heterostructures requires quantitative characterization and understanding of these various interactions and tailoring of spin-orbit interactions.

３．研究の方法

The current research project is directed towards the quantification of current-driven DW dynamics in AFM/FM and realization of current-induced switching of AFM/non-magnet (NM) structures for AFM-based neuromorphic computing architectures. The project has been divided into four different activities for systematic investigations of current-induced effects in these structures.

(1) Growth of AFM/FM heterostructures:
The first step was directed towards the optimization of ultrathin film of AFM/FM and AFM/NM structures. Mn-based room temperature AFM alloy $Pt_{0.38}Mn_{0.62}$ was deposited by magnetron sputtering on high-resistive Si substrates with Ta/Pt/MgO buffer layers. For AFM/FM structures, Co/Ni multilayer was grown on top of the AFM layer and capped with MgO/Ru. For AFM/NM structures, Pt or Ta was grown above the AFM layer and capped with MgO/Ru. The growth conditions of the various layers were determined from X-ray reflectivity measurements. Crystalline orientation of the blanket films was determined from X-ray diffraction (XRD) and transmission electron microscopy (TEM) measurements. Subsequent M-H measurements at room temperature indicates the prevalence of an exchange bias in PtMn/FM structures supportive of the AFM nature of the PtMn.

(2) Fabrication of μm & nm-sized AFM/FM devices for characterization of SOTs and DW motion:
(a) SOTs in AFM/FM heterostructures: Electrical transport properties of thin films are probed using Hall bar structures. We utilize dc-magnetotransport measurements for the quantification of SOT-induced effective fields arising from the injection of current. Starting from a saturated magnetized state, we measure Hall resistance (R_H) as a function of the applied magnetic field angle (ϕ). Analysis of the experimental data considering the planar Hall and anomalous Hall contributions of R_H enables the quantification of SOT-induced effective fields in the PtMn-based AFM/FM heterostructures. PtMn thickness (t_{PtMn}) dependence of SOT-induced effective field measurements were carried out to obtain deeper insights into the nature of spin-orbit interaction in these heterostructures.
(b) Current-induced DW motion in AFM/FM structures: The magnetic ordering in systems with broken inversion symmetry is sensitive to interfacial spin-orbit interactions, referred to as Dzyaloshinskii-Moriya interaction (DMI). The presence of DMI renders the stabilization of chiral spin textures, fast SOT-driven DW motion and generation of skyrmions. An investigation of DMI is thus essential concerning the potential application of AFM/FM heterostructures. We utilized nm-sized Hall bar devices fabricated by electron-beam lithography and Ar ion milling for quantification of current-induced DW motion in AFM/FM heterostructures. The presence of DMI acts as an effective longitudinal magnetic field (H_{DMI}) stabilizing homochiral Néel DWs. An applied in-plane magnetic field (H_X) either stabilizes or destabilizes the Néel configuration resulting in a modulation

of DW velocity (v). For, $H_K = H_{DMI}$, v equals zero. Our experimental results on current-induced DW motion enables the quantification of H_{DMI} and enables the understanding of DW motion in AFM/FM heterostructures.

(3) Magneto-resistive effects at AFM/NM heterostructures:

One of the pertinent questions concerning the realization of pure antiferromagnetic spintronics is an electrical detection of antiferromagnetic moments without macroscopic magnetization. Recent studies have revealed that the interaction of current with antiferromagnetic moments leads to several magnetoresistive effects serving as an electrical probe for detection. As a result, quantification of magnetoresistive behaviors in antiferromagnetic systems have gained considerable interest. We utilize substrate/ Ta(3)/ Pt(3)/ MgO(2)/ $Pt_{0.38}Mn_{0.62}(1 \leq t_{PtMn} \leq 10)$/ Pt(5)/ Ru(1) for quantification of magnetoresistive effects, (numbers in parentheses are the nominal thickness in nm). Angle dependent magnetoresistance (ADMR) measurements are carried out for the fabricated structures in a four-probe configuration using a current reversal technique. Longitudinal voltages (V_{XX}) are measured under an applied current (I_{DC}) for H rotations along x-y, y-z and x-z axes from which longitudinal resistances (R_{XX}) are calculated by averaging the voltages for positive and negative currents.

(4) Current-induced manipulation of an antiferromagnet:

An important question for realization of AFM-based spintronic architectures concerns electrical control of antiferromagnetic moments. We demonstrate SOT-induced control of antiferromagnetic moments in sub./Ta(3)/Pt(3)/MgO(2)/$Pt_{0.38}Mn_{0.62}(10 \leq t_{PtMn} \leq 30)$/Pt(5)/Ru(1), where the numbers in parentheses are the nominal thickness in nm (Fig. 1(a)). The obtained results are compared to reference structure sub./Ta(3)/Pt(3)/MgO(2)/$Pt_{0.38}Mn_{0.62}(10 \leq t_{PtMn} \leq 30)$/Ru(1). The deposited films are patterned into star-shaped structures by photolithography and Ar ion milling. After fabrication, the structures are annealed in an in-plane magnetic field of 1.2 T for 2h. at 300 °C applied collinear to the channel. Electrical writing of information was achieved by sourcing pulsed currents along two orthogonal directions (I_{Write}^1 and I_{Write}^2) while reading of the corresponding resistance state was achieved by measuring the transverse Hall resistance (R_{Hall}) of the sample under an applied dc (I_{Read})

4. 研究成果

(1) Quantification of SOTs in AFM PtMn(t_{PtMn})/FM heterostructure:

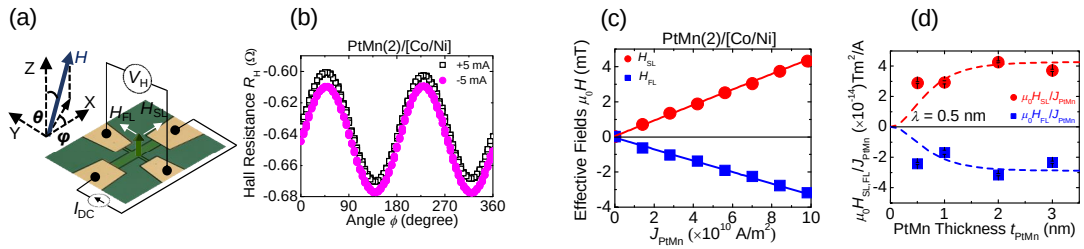

Figure1: (a) Schematic diagram of experimental set-up and definition of axes of external field (H) with an optical micrograph of a typical device. (b)Measured Hall resistance (R_H) vs angle (ϕ) in X-Y plane for a fixed magnitude of 400 mT for PtMn(2)/[Co/Ni].(c) Current-induced effective fields (H_{SL} and H_{FL}) vs current density in underlayer (J_{PtMn}) for PtMn(2)/[Co/Ni].(d) Effective fields per unit current density vs PtMn thickness for PtMn/[Co/Ni]. Broken curves are fitting based on a drift-diffusion model.

The injection of current in the AFM results in longitudinal or Slonczewskii-like (H_{SL}) and transverse or field-like (H_{FL}) SOT-induced effective fields acting on the adjacent ferromagnetic layer. Figure 1(a),(b) show the measured R_H vs ϕ under $I_{DC} = \pm$ 5 mA for PtMn(2)/[Co/Ni] structures. Considering the anomalous Hall and planar Hall contributions to R_H, we use the difference between $R_H(\phi)$ for $+I_{DC}$ and $-I_{DC}$ to derive H_{SL} and H_{FL}. Same experiment is repeated with different I_{DC} ($0 \leq |I_{DC}| \leq 10$ mA). As the bulk spin Hall effect (SHE) of the underlayer (PtMn) is considered to be a major factor in the observed SOT, we plot the obtained H_{SL} and H_{FL} versus current density in PtMn (J_{PtMn}) Fig. 1(c). A linear relation is observed, indicating that the observed effective fields are induced by the applied current. The underlayer thickness dependence of effective fields per unit current density determined from a linear fitting is summarized in Figs. 1(d). The observed sign of H_{SL} corresponds to a positive spin Hall angle in the AFM PtMn. According to the scenario that SOT originates from SHE, underlayer thickness dependence of the effective fields can be described by a drift-diffusion model $H_{SL,FL} \propto (1\text{-sech}(t_{PtMn}/\lambda_{PtMn}))$, where λ_{PtMn} represents the spin-diffusion length. The fitting curves in Figs. 1(d) with $\lambda_{PtMn} = 0.5$

nm reasonably describes the result [4]. Finally, we can also determine the effective spin Hall angle θ_{SH}^{eff} from $\theta_{SH}^{eff} = 2eM_S t_F H_{SL}/\hbar J_{PtMn}$ (t_F is ferromagnetic layer thickness) to be 0.19 ± 0.03 for PtMn.The dc-magnetotransport measurements of SOT-induced effective fields indicate significant SOT-induced effective fields with a positive sign of spin Hall angle for AFM-based PtMn/[Co/Ni] structures.

(2) Current-induced DW motion in AFM/FM PtMn/[Co/Ni] heterostructures:

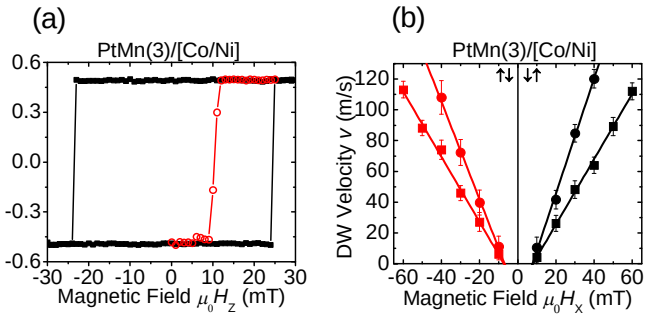

Figure2:(a) Hall resistance (R_H) vs out-of-plane magnetic field (H_Z) without (black squares) and with (red circles) the creation of DW for PtMn(3)/[Co/Ni]. (b) DW velocity (v) vs in-plane magnetic field (H_X) for up-down ↑↓ and down-up ↓↑ configurations under two different current densities for PtMn(3)/[Co/Ni]. Correspondence between symbol and current density is as follows-squares (circles); J_{PtMn} = 6.4 × 10^{11} A/m² (7.4 × 10^{11} A/m²). Solid lines are linear fit.

Current-induced DW motion experiments were carried out in nm-sized DW motion conduits fabricated by e-beam lithography and Ar ion milling. Figures 2(a) show R_H-H_Z curves for PtMn/[Co/Ni] structure. The field inducing reversal of the nanowires without DW, representing a nucleation field, is 25 mT for PtMn/[Co/Ni],while, the DW propagation field, measured after creating DW using an orthogonal Oersted line, is 10 ± 2 mT. Next, H_X dependence of CIDWM is measured at a constant current with 10-ns pulse width for both domain configurations (up-down ↑↓ and down-up ↓↑). The experiment is repeated for different magnitudes of the current for each H_X. Figures 2(b) show v vs H_X for two different current densities J for the PtMn/[Co/Ni]. Under an applied J and H_X, ↑↓ and ↓↑ DWs move along current direction, signifying SOT-induced DW motion. The results indicate that DWs in PtMn/Co possess a right-handed chirality (↑→↓←↑). According to a one-dimensional model for DW motion by SHE, DMI constant (D) can be determined from H_S as[4,5,8,18] $H_S = \varepsilon [D + (2.1 \times 10^{-4}) \text{sign}(\theta_{SH}) P |J_{FM}|]/M_S \Delta$, where sign($\theta_{SH}$) represents the sign of θ_{SH}^{eff} (> 0 for both PtMn and Pt), P is the spin polarization of current flowing in the FM layer, J_{FM} represents current density in FM layer, $\varepsilon = \pm 1$ depending on the type of DW, and $\Delta = (A/K_{eff})^{1/2}$. Linear fitting yields $\mu_0 H_S$ = 7.6 ± 0.7 Mt for PtMn/[Co/Ni]. Subsequently, for P = 0, we obtain, D = +0.042 ± 0.004 mJ/m² for PtMn/[Co/Ni] system. The present results unambiguously indicate the existence of DMI arising from the AFM/FM interface in PtMn/[Co/Ni] system [4].

(3) Angle-dependent magnetoresistive effects at AFM/NM structure:

Figures 3(a)-(c) shows the schematics of measurement process while Figs. 3(d)-(i) show the polar plot of ADMR for applied $\mu_0 H$ = 2, 4 and 6 T (μ_0 is the permeability in free space) rotated along θ_{XY}, θ_{YZ} and θ_{XZ} for PtMn(1)/Pt and PtMn(10)/Pt, respectively. Amplitude of longitudinal magnetoresistance (MR_{XX}) indicate a finite value of MR_{XX} both for PtMn(1 and 10)/Pt and PtMn(10)/W along all three rotation planes with a two-fold symmetry over the full angle of rotation. The functional dependence of ADMR, indicated by continuous lines in Figs. 3(d)-(i), however, shows marked variation with the increase of t_{PtMn}. For PtMn(1)/Pt, ADMR along ADMR along θ_{XY} and θ_{YZ} follows Cos(θ_{XY}) and Sin (θ_{YZ}) dependence, respectively. Interestingly, an increase of t_{PtMn} to 10 nm results in a transformation of the observed behavior to Sin (θ_{XY}) and Cos(θ_{YZ}), respectively. A comparison of the obtained magnitude of MR_{XX} for PtMn(10)/Pt indicates a spin-Hall magnetoresistive effect leading to the observed magnetoresistive behavior. Our experimental results show the existence of appreciable magnetoresistance in this hitherto unexplored AFM metallic bilayer systems, and bears promise for detection of AFM dynamics under applied perturbations in metallic heterostructures [5].

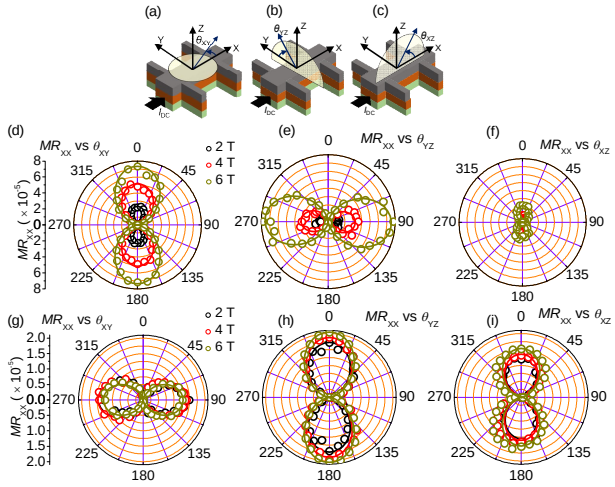

Figure3:(a)-(c) Schematic diagram of experimental set-up and definition of the mutually perpendicular H rotation planes with angles θ_{XY}, θ_{YZ} and θ_{XZ}, respectively. (d)-(f) Polar plot of angle dependent magnetoresistance (ADMR) measurements along angles θ_{XY}, θ_{YZ} and θ_{XZ}, respectively under an applied field $\mu_0 H$ = 2, 4 and 6 T for PtMn(1)/Pt(5) structure. (g)- (i) shows the results of same experiment for PtMn(10)/Pt(5) structure.

4. Current-induced manipulation of AFM/NM structure:

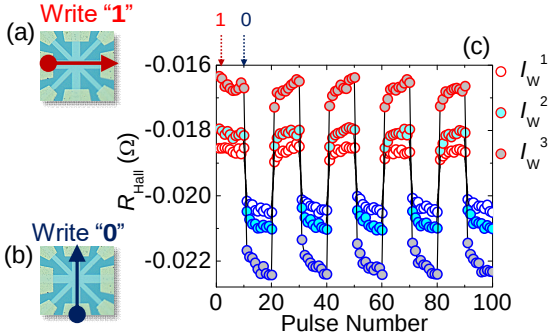

Figure 4: (a), (b) shows device structure and schematic of current-induced writing process. Write 1 denotes horizontal current-pulse application and write 0 is achieved by applying vertical current-pulse. (c) experimental results of electrical manipulation of AFM/NM under orthogonal write currents. I_W^1, I_W^2, I_W^3 ($I_W^1 < I_W^2 < I_W^3$) corresponds to applied current-pulse magnitude while R_{Hall} is the measured Hall resistance.

Capability of utilization of antiferromagnets (AFMs) as multifunctional components of spintronic devices has opened new directions in the field of next generation low power consuming spintronic architectures. The absence of a net magnetic moment, intrinsic ultrafast dynamics and higher packing density in these class of materials entails promising characteristics useful for next generation non-volatile AFM memory architectures, multi-level analogue bit cell for neuromorphic applications, AFM/ferromagnet (FM)-based neuron and synapses and skyrmion-based computing. The complete potential of antiferromagnetic spintronics, however, relies on the realization of (ferro)-magnet free AFM based spintronic devices capable of complementing current FM-based architectures. Figure 4(a), (b) shows the schematic diagram of writing procedure under the application of orthogonal write current pulses of milli-sec duration and varying pulse amplitudes (I_W^1, I_W^2, I_W^3). The application of write 1 pulse result in a high-resistive state while write 0 corresponds to a low resistive state respectively, indicative of current-induced manipulation of the AFM (Fig. 4(c)). The amplitude of the bi-stable resistive nature increases with an increasing magnitude of write current and can be controllably reversed under current-pulse polarity reversal, indicative of SOT-induced manipulation of the AFM by spin-current injection from the NM layer. Separate experiments (not shown here) on single-layer AFM PtMn reveals negligible changes in resistance under the injection of similar current in the AFM, supportive of SOT-induced manipulation of the AFM. The results of the electrical experiments are further supported by X-ray linear magnetic imaging of the AFM under the action of SOTs. Our experimental results direct towards the possibility of utilization of SOT-induced manipulation of AFM/NM structures for antiferromagnetic spintronic architectures.

References:
(1) S. Fukami, S. DuttaGupta *et al.*, *Nature Mat.* **15**, 535 (2016)
(2) A. Kurenkov, S. DuttaGupta *et al.*, *Advanced Materials* 1900636 (2019)
(3) A. Kurenkov, S. DuttaGupta, *et al.*, *Appl. Phys. Lett.* **110**, 092410 (2017)
(4) S. DuttaGupta, *et al.*, *Appl. Phys. Lett.* **111**, 182412 (2017)
(5) S. DuttaGupta, *et al.*, *Applied Physics Letters* **113**, 202404 (2018)

５．主な発表論文等

〔雑誌論文〕（計 3 件）

Published:

1. T. Dohi, S. DuttaGupta, S. Fukami and H. Ohno, Reversal of domain wall chirality with ferromagnet thickness in W/(Co)FeB/MgO systems, *Applied Physics Letters* **114**, 042405 (2019) (**refereed**).
2. S. DuttaGupta, R. Itoh, S. Fukami and H. Ohno, Angle dependent magnetoresistance in heterostructures with antiferromagnetic and non-magnetic metals, *Applied Physics Letters* **113**, 202404 (2018) (**refereed**).
3. S. DuttaGupta, T. Kanemura, C. Zhang, A. Kurenkov, S. Fukami and H. Ohno, Spin-orbit torques and Dzyaloshinskii-Moriya interaction in PtMn/[Co/Ni] heterostructures, *Applied Physics Letters* **111**, 182412 (2017) (**refereed**).

〔学会発表〕（計 8 件）

1. S. DuttaGupta, R. Itoh, A. Kurenkov, S. Fukami and H. Ohno, *"Spin Hall Magnetoresistance in antiferromagnet/nonmagnet metallic structures"*, York-Tohoku-Kaiserslautern Symposium on "New-Concept Spintronic Devices", June 12-14th 2019, University of York, England (invited).
2. S. DuttaGupta, R. Itoh, S. Fukami and H. Ohno, "Angular dependence of longitudinal and transverse magnetoresistance in antiferromagnet/nonmagnet metallic heterostructures", 16th RIEC International Workshop on Spintronics and 8th JSPS Core-to-Core Workshop on "New-Concept Spintronic Devices", 9th-12th January 2019, Tohoku University, Sendai, Japan.
3. S. DuttaGupta, A. Kurenkov, R. Itoh, S. Fukami and H. Ohno, "*Angle dependent magnetoresistance in nonmagnet/antiferromagnet metallic heterostructures*", 9th Joint European Magnetic Symposium (JEMS) Conference 2018, 3rd- 7th September 2018, Mainz, Germany.
4. S. DuttaGupta, A. Kurenkov, R. Itoh, A. Okada, S. Fukami and H. Ohno, "*Angular dependence of magnetoresistance in antiferromagnet-nonmagnet bilayer structure*", Tohoku-Tsinghua Joint Workshop on Materials and Spintronics Sciences, July 26th 2018, Sendai, Japan (invited).
5. S. DuttaGupta, A. Kurenkov, R. Itoh, A. Okada, S. Fukami and H. Ohno, "*Angle dependent magnetoresistance in nonmagnet/antiferromagnet metallic heterostructure*", International Conference on Magnetism (ICM) 2018, July 15th- 20th 2018, Moscone Center, San Francisco, USA.
6. S. DuttaGupta, T. Kanemura, R. Itoh, A. Kurenkov, C. Zhang, S. Fukami and H. Ohno, "*Dzyaloshinskii-Moriya interaction in an antiferromagnet/ferromagnet heterostructure*", The 65th JSAP Spring Meeting, March 17th- 20th 2018, Waseda University, Tokyo, Japan.
7. S. DuttaGupta, A. Kurenkov, R. Itoh, C. Zhang, S. Fukami and H. Ohno, "*Magnetoresistance in a nonmagnet/antiferromagnet metallic heterostructure*", The 65th JSAP Spring Meeting, March 17th- 20th 2018, Waseda University, Tokyo, Japan.
8. S. DuttaGupta, T. Kanemura, A. Kurenkov, C. Zhang, S. Fukami and H. Ohno, "*Characterization of spin-orbit torque and Dzyaloshinskii-Moriya interaction in an antiferromagnet/ferromagnet structure*", The 62nd Annual Conference on Magnetism and Magnetic Materials, November 6th -10th 2017, Pittsburgh, USA.